Inoculant enhancer to increase the potency of Ca-FeSi alloy in ductile iron produced from the low rare earth containing master alloy

I. Riposan[1*], V. Uta[1], S. Stan[1], M. Chisamera[1], M. Firican[1], R. Naro[2], D. Williams[2]
[1]POLITEHNICA University of Bucharest, Bucharest, Romania
[2]ASI INTERNATIONAL LTD, Cleveland, Ohio, USA

The world rare earth elements [REE] crisis will continue at least in the short and medium term. With less REE available, their future use in foundry alloys should be carefully thought out and other inoculation methods need to be investigated. The use of an inoculant enhancer [OS-IE] led to a substantial increase in the potency of a 75% Ca-bearing FeSi alloy in low REE produced ductile irons, as this [Ca-FeSi + OS-IE] inoculation variant led to the lowest chill tendency, the highest nodule count and graphite nodularity. This combination of inoculant was more effective than an equivalent addition of 1) a REE-bearing, Ca-FeSi alloy, or 2.) a Ca,Ba-FeSi alloy, or 3.) the standard Ca-FeSi alloy variant, but with 60% or 77% lower alloy consumption, respectively. The enhancement of the 75% Ca-bearing FeSi alloy by the contribution of an addition of sulphur, oxygen and oxide-forming elements, appears to be a better and more effective inoculation solution compared to using more expensive inoculating elements, such as the REE or Ba containing alloys.

Keywords: ductile iron, magnesium, rare earths, inoculant enhancer, in-mould inoculation, chill, graphite nodularity, nodule count, shape factors

Introduction

Oxy-sulphide forming elements appear to have a very important role in graphite nucleation in cast irons. Complex (Mn,X)S compounds (where X = Fe, Al, O, Ca, Si, Sr, Ti, Zr, etc.) nucleated on Al_2O_3-based sites[1-5] and were the primary sites for graphite flake growth in both un-inoculated and inoculated grey irons (Fig. 1a).[4] Generally considered as inoculating elements, calcium and strontium were found to distribute differently in the inclusion volume. Calcium was distributed evenly throughout the inclusion while strontium was found mainly in the core of the inclusions. Particles associated with graphite had a lower Mn/S ratio than the matrix-embedded particles. The Ca-FeSi and Sr-FeSi inoculated irons had a lower Mn/S ratio than high-purity (HP) FeSi treated irons.[1-5]

According to M.H. Jacobs et al,[6] graphite nodules nucleate heterogeneously on particles formed in the melt, and exhibited a duplex sulphide/oxide structure. These nucleating particles consisted of a central seed, surrounded by an outer shell of different crystal structure and chemical composition. For Ca-FeSi and Sr-FeSi inoculated, FeSiMg treated iron, it was found that the central seed consisted of (Ca,Mg)S *versus* (Sr,Ca,Mg)S compounds, while the outer shell was a (Mg,Al,Si,Ti)Oxide having a spinel structure. It appears that Mg, Ca, and Sr play two important roles in ductile iron nucleation: 1) to combine with and remove the free S from the melt and 2) to form of sulphide particles, both roles

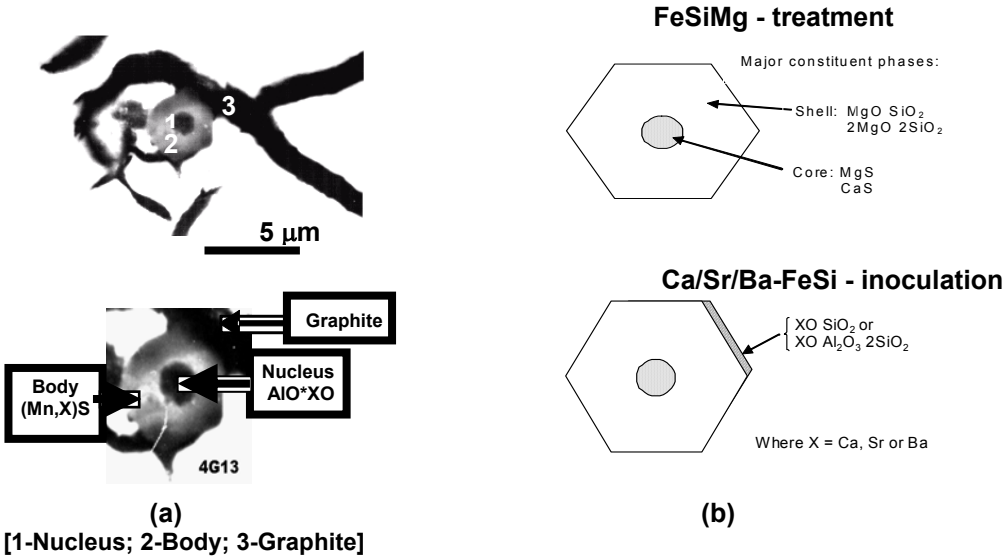

Fig. 1: Graphite nucleation mechanism in grey iron (a)[4] and ductile iron (b)[7]

* Corresponding author, email: i_riposan@rectorat.pub.ro

being important and necessary steps in graphite nucleation. T. Skaland found complex hexagonal silicate phases of XO-SiO_2 or XO-Al_2O_3-$2SiO_2$ on the surface of the previously formed Mg-silicates (Fig. 1b) making them more favourable sites for subsequent graphite nucleation. In post-inoculated ductile irons, X can be either Ca, Ba, or Sr. All of these phases will serve as favored sites for graphite inoculation.[7]

The simultaneous addition of sulphur with potent oxy-sulphide forming elements was first demonstrated by Naro and Wallace,[8] who showed that balanced ratios of rare earths and sulphur, without the presence of ferrosilicon, drastically reduced undercooling, completely eliminated chill and promoted favorable graphite shapes in grey irons (Fig. 2). Strande[9] showed that using CaSi-based inoculants along with increased direct sulphur additions to the metal vastly improved machinability in grey iron castings. Chisamera and Riposan[1-5] also illustrated the importance of sulphur content and inoculant effectiveness in grey irons.

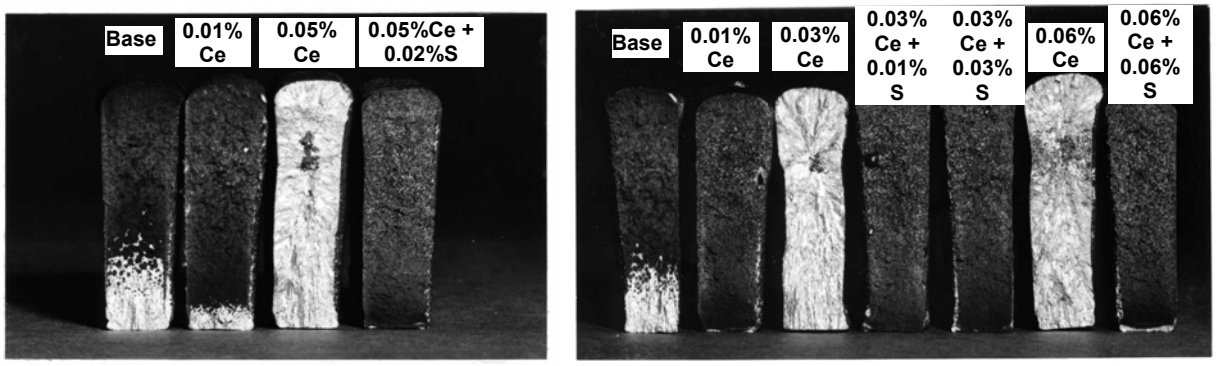

Fig. 2: Effect of oxy-sulphide forming elements (Ce and S) on the chilling tendency of grey iron[8]

In ductile irons, Chisamera and Riposan[10-14] demonstrated that less than 0.01wt.%S added concurrently with CaSi-based inoculants or/and rare earth elements, increased graphite-nucleation potential without affecting graphite nodularity. It was found that the strong sulphide-forming tendencies of Ca and rare earth, when used with controlled sulphur additions, strongly promoted the formation of sulphide compounds, assisting in their effectiveness as nodular graphite nuclei. Later, Skaland[15,16] developed an inoculant concept based on adding small and controlled amounts of sulphur and oxygen coated onto the surface of a Ca/Ce-FeSi alloy that could react with calcium and cerium when introduced into liquid iron.

Aluminum also appears to play an important role in nodular graphite nucleation in ductile irons. Aluminum has been found in nodular graphite as a complex nitride, such as AlMg2.5Si2.5N[17] and (Mg, Si, Al)N,[18] and as an oxy-nitride (Mg, Si,Al)ON at very low sulphur contents in the base iron (< 0.01wt.% S).[19] Aluminum, together with Mg and Ca as a constituent in sulphide and silicate inclusions has been observed in induction and cupola melted iron.[20] Recent work has also shown that a specific low level of aluminum has a beneficial impact on the properties of ductile iron.[21-23]

To exploit the important role that S, O, Al and oxy-forming elements play in the nucleation of graphite, new complex alloys have been developed.[24-25] These alloys contain potent nuclei (or oxy-sulphide) forming elements in a concentrated, easy-to-use form. They contain up to 20 times the level of oxy-sulphide forming elements normally found in other ladle or in-stream inoculants, or in cast and/or sintered in-mould inserts. They are useful as a solo inoculant or can be added as separate additions with conventional inoculants, acting as an inoculant enhancer, to increase the potency of Ca-FeSi alloys. As a result, greater efficiencies during inoculation treatment have been obtained at significantly lower addition rates, in both grey iron[26] and ductile irons.[27-29]

Generally, rare earth elements (REE) are used in ductile iron to 1.) neutralize tramp elements that interfere with the nodulizing effect of Mg, 2.) assist in nodulizing by providing a supplementary boost to Mg and lastly, 3.) assist in the inoculation effect of nucleating graphite. The use of REE's and the amount needed is dependent on charge materials quality and castings requirements. The unique properties of REE have caused them to be crucial to a number of emerging, growing technologies, as REE are important and critical to hundreds of other high-tech, non-foundry applications. The world REE crisis will continue, at least in the short and medium term, and less REE will be available for use in cast iron graphite morphology control, and their future foundry use must be carefully considered.[28,29]

A previous paper[28] pointed out that the anti-nodularising action of residual elements up to a level corresponding to a Thielman factor K[30] equaling 2.0 could be counteracted by REE additions. Such additions could also be beneficial for K values less than 1.2 and in some applications, can be regarded as compulsory for K values greater than 1.2. On the other hand, it was found that in relatively pure base iron with lower anti-nodularising trace elements (having Thielman Factor K less than 0.8), the microstructure was affected by solidification cooling rate, REE_{res} content, post-Mg-treatment and inoculant type. Without the role to neutralize the anti-nodularising trace elements, increased REE_{res} contents from 0.005 up to 0.025% increased carbide tendency and decreased nodular graphite compactness degree.[28,29]

The main objective of the present paper is to examine the effects of in-mould inoculation, using commercially available FeSi-based inoculants, in relatively pure base irons having low levels of anti-nodularising trace elements

(Thielman Factor K less than 0.8) and less than 0.01%REE_{res} (produced from the low REE-containing master alloy). Another inoculation variant consisted of adding a proprietary oxy-sulphide inoculant enhancing alloy [(OS-IE) based on a patented blend of CaSi, Al and proprietary oxy-sulphide elements][24] to a conventional Ca-bearing 75% FeSi alloy.

Experimental Procedure

The experimental heat was melted in an acidic refractory lined, coreless induction furnace (100kg, 2400Hz). The base iron melt was heated to 1500-1520^{0}C and then tapped into a 30kg nodulizing ladle. A tundish cover Mg-treatment technique was used along with a 2.5 wt.% Mg-bearing FeSi master alloy [wt.%: 44.7Si, 5.99Mg, 1.02Ca, 0.26TRE-Total Rare Earth (0.15Ce, 0.11La, 0.008Nd), 0.91Al, 0.35Mn, 0.048Ti, 0.10Cr, 0.035Ba, balance Fe] addition.

Three commonly used post-inoculants were evaluated, 1.) Ca-FeSi, 2.) Ca,Ba-FeSi and 3.) Ca,RE-FeSi, all having similar Si (72.6-73.8wt.%), Ca (0.87-1.02wt.%) and Al (0.77-0.96wt.%) levels. The main difference was the presence of 1.68wt.%Ba or 1.86wt.%TRE (Total Rare Earth), respectively, compared to the Ca bearing FeSi alloys. The above inoculants were added to an in-mould reaction chamber. After careful consideration of typical addition rates for in-mould, ductile iron inoculation, (typically 0.04 to 0.20wt.%), different inoculants consumptions were selected, depending on their presumed inoculating ability: 1.) 0.18wt.%Ca-FeSi, 2.) 0.10wt.%Ca,Ba-FeSi and 3.) 0.04wt.%CaRE-FeSi. Another inoculation variant consisted of adding an oxy-sulphide inoculant enhancing alloy [(OS-IE) based on a proprietary, stoichiometric blend of CaSi, Al, Mg and oxy-sulphide elements].[24] The inoculant enhancer was added as a separate addition to the reaction chamber with 75% Ca-bearing FeSi at the following rate: standard Ca-bearing 75% FeSi at 0.03 wt.% consumption level (75%) and Inoculant Enhancer (OS-IE) at 0.01 wt.% consumption level (25%), or more simply, a 3 to 1 ratio.

The specially designed test mould included a central downsprue, which supplied Mg-treated iron simultaneously to four separate reaction test chambers (one as an un-inoculated reference and three to test the different alloys).[28,29] W_3 chill wedge samples [ASTM A367-85 specification, 19.1 x 38.1 x 101.6 mm) dimensions, CM = 3.5 mm cooling modulus], plate specimens (4.5mm thickness) and round bar cooling specimens (25mm diameter) were gated off the inoculation reaction chamber. This allowed for evaluation of chemistry and microstructure characteristics after treating the ductile irons with the different inoculants [using 1450^{0}C pouring temperatures, pouring 3 minutes after Mg-treatment, into furan resin bonded moulds].

The wedge test samples were used to evaluate the influence of cooling rate on the structural characteristics of un-inoculated and inoculated irons. These samples were polished to determine graphite parameters on un-etched samples and then etched with Nital to determine free carbide percentages and the ratio of pearlite/ferrite. The structure variation on the centerline direction from the apex up to the base of wedge sample was evaluated at three points (the center and 1.0 mm distance left and right of the centerline). For each distance from the apex, the following conditions were used: 5μm trap size, 100x magnification, 3 fields were analyzed (more than 500 nodules) and the averages of the structure parameters were determined. The graphite characteristics were evaluated with Automatic Image Analysis [analySIS® FIVE Digital Imaging Solutions software].

$$\text{Sphericity Shape Factor (SSF)} = 4\pi A_G / P_G^2 \qquad \text{Equation 1}$$

$$\text{Graphite Nodularity (NG-SSF)} = 100\,[\Sigma A_{\text{particles-SSF}} / \Sigma A_{\text{all particles}}] \qquad \text{Equation 2}$$

Where:

$A_{\text{all particles}}$ is the area of all graphite particles greater than 5 μm; $A_{\text{particles-SSF}}$ is the area of particles for a specific SSF range; A_G is the area of the graphite particle in question; and P_G is the real perimeter of the graphite particle in question [the sum of the pixel distances along the closed boundary].

Results and Discussion

The final composition of the ductile irons (wt.%: 3.20-3.45C, 2.6-2.7Si, 0.57-0.64Mn, 0.016-0.017S, 0.0165-0.0182Al, 0.046-0.058Mg, 0.0045-0.0054Ce, 0.0010-0.0014La) lies solidly in the eutectic range, expressed by carbon equivalent (CE values between 4.1-4.4%) and carbon saturation degree (S_c values between 0.95-1.02). Typically, these irons have relatively low anti-nodularising Thielman factors (K values between 0.6 to 0.8) and a medium level of pearlite promoting factor P_x values between 2.2 to 2.5.[30] It was determined that the content of anti-nodularising elements in both Mg-treated irons was so low (K values less than 0.8), that the role of rare earths to counteract these elements was not necessary. The pearlite factor P_x, for conventional solidification conditions, would indicate a pearlite forming tendency.

The metal matrix and graphite phase characteristics are affected by the following: the solidification cooling rate (as the distance from the apex of wedge castings increases, corresponding to wall thickness increasing, the cooling rate is reduced); post-Mg-treatment application (un-inoculated versus inoculated ductile irons); inoculant type.

Examination of all chill wedges showed that free carbides were mainly present in the wedge sample apex area (Fig. 3), which solidified at the highest cooling rate, independently of the ductile iron state (un-inoculated or inoculated), and inoculating element type. As the distance from the apex increases, cooling rates decrease, leading to important changes in the solidification pattern, duly noting all of the other influencing factors that are important contributors to stable or

meta-stable solidification conditions. Typically, larger amounts of free carbides in un-inoculated irons occurred, with the amount decreasing as the distance from the apex increases. The presence of free carbides was avoided only when the wedge casting section thicknesses was greater than 10mm (more than 20mm distance from the apex).

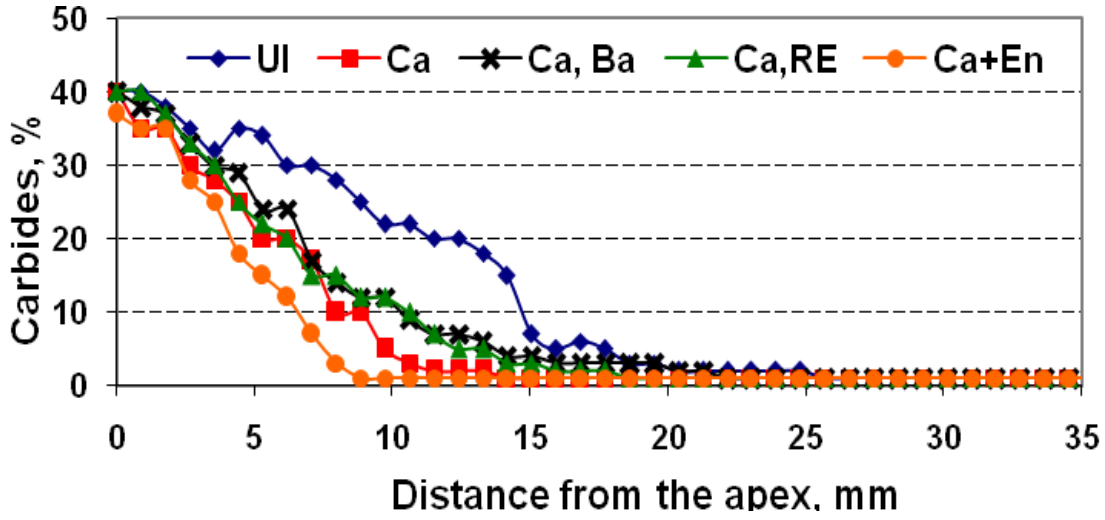

Fig. 3: Influence of the distance from the apex [W_3 wedge samples, ASTM A367] and inoculating elements on the carbides amount, in tested ductile irons [UI – un-inoculated; Inoculation: Ca – 0.18%Ca-FeSi; Ca,Ba – 0.10%Ca,Ba-FeSi; Ca,RE – 0.04%Ca,RE-FeSi; Ca+En – 0.04% [3/4Ca-FeSi + ¼ Enhancer (OS-IE)]

Inoculation of all the ductile irons decreased the carbide forming sensitivity, but at different magnitudes, depending on inoculant type and consumption level. All of the modified Ca-bearing FeSi alloys show improved inoculation capability, and incorporating either Ba or REE in the alloys contributed to increased inoculating potency. These active elements allowed a lower consumption level of inoculants, namely allowing the use of 0.10wt.%Ca,Ba-FeSi or 0.04wt.%Ca, RE-FeSi; the chill tendency was essentially at the same level as when standard additions of 0.18wt.%Ca-FeSi were made.

The use of the inoculating enhancer [OS-IE] significantly increased the effectiveness of the standard Ca-bearing FeSi alloy. The [Ca-FeSi + Enhancer] inoculation variant led to the lowest chill tendency. When compared to Ca,Ba-FeSi variant, 60% less alloy was needed to obtain the same chill reduction (0.10wt.% versus 0.04wt.%). When compared to the standard Ca-FeSi variant used by itself, 77% less alloy was needed to obtain the same level of chill reduction (0.18wt.% versus 0.04wt.%). The combination of [Ca-FeSi + Enhancer] was also more effective than an equivalent addition of the REE-bearing Ca-FeSi alloyed used at the 0.04wt.% level.

The metal matrix of W_3-ASTM A367 samples was mainly pearlitic (more than 90% pearlite), as predicted by the P_x factor (P_x = 2.2 to 2.5) for all of the tested irons. Although ferrite formation is favoured by lowering the cooling rate (thicker wall section castings), the amount of ferrite that formed was also dependent on the inoculation variants. All inoculated ductile irons showed a larger amount of ferrite, compared to un-inoculated irons. When comparing inoculation capability, the [Ca-FeSi + OS-IE Enhancer] variant appeared to have the greatest ferrite forming effect (starting at 5mm wedge casting section size), despite being used at the lowest consumption level.

Figure 4a shows a general view on the graphite phase, at different distances from the apex of wedge sample, or casting section size. Graphite particles are clearly visible in un-inoculated irons when the section size was in the range of 1.0 to 2.0mm [or 1.6-3.0mm distance from the apex]. With these very high solidification cooling rates, all of the inoculant variants led to increased graphite amounts and nodule counts. This was especially true for the 0.18wt.% [Ca-FeSi] variant, but also for the 0.04wt.% [(Ca-FeSi + (OS-IE)] alloy variant, again noting that it was used at a 77% lower consumption level.

As the cooling rate decreased and as the distance from the apex and the section size increased, increasing amounts of graphite formed in both the un-inoculated and inoculated irons. The largest difference in graphite percentage and nodule count was observed when the distance from the apex was 10 to 12 mm (corresponding to a section size of 5-6mm) or corresponding to thin walled castings having wall thicknesses of 5 to 6 mm (Figures 4b and 4c). When the distance from the apex was 10 to 12 mm, the large addition of the Ca-bearing FeSi alloy (0.18wt.%Ca-FeSi) resulted in the lowest carbide levels, and the highest graphite amounts and nodule counts. Although the 0.10wt.%Ca,Ba-FeSi and 0.04wt.%Ca, RE-FeSi inoculant variants were used at significantly reduced consumption levels, the beneficial effects of Ba and REE were only modest at these addition levels.

For the upper part of W_3 wedge casting, when the distance from the apex was more than 20mm, [corresponding to a section size greater than 10mm], the presence of free carbides was essentially eliminated in all of irons. The graphite amount was relatively constant at 8 to 10%, with minimal or limited effects of inoculant type and consumption.

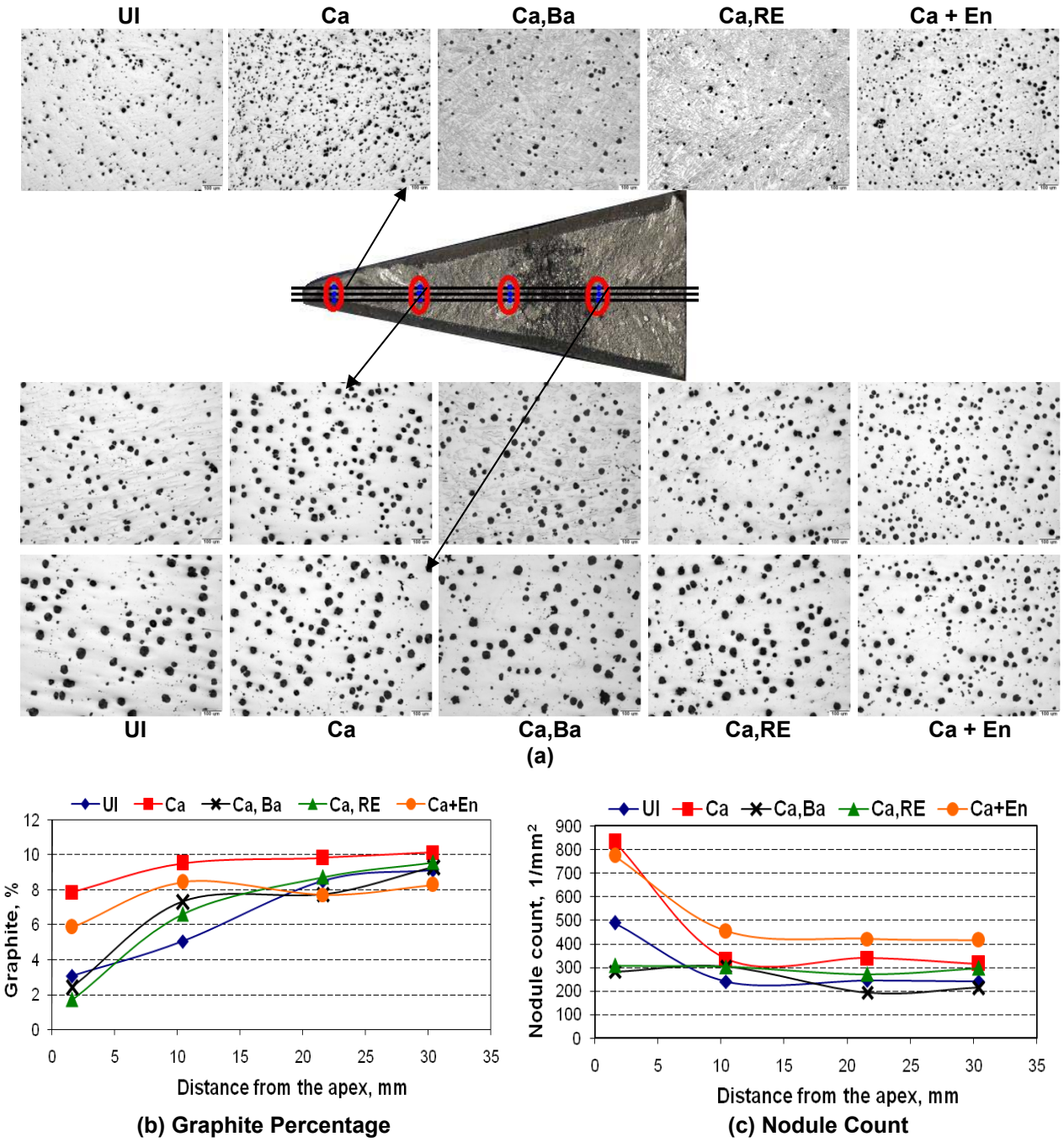

Fig. 4: Influence of the distance from the apex [W_3 wedge, ASTM A367] and inoculating elements on the structure (a), graphite amount (b) and nodule count (c), in tested ductile irons [UI – un-inoculated; Inoculation: Ca – 0.18%Ca-FeSi; Ca,Ba – 0.10%Ca,Ba-FeSi; Ca,RE – 0.04%Ca,RE-FeSi; Ca+En – 0.04% [0.75 Ca-FeSi + 0.25 Enhancer (OS-IE)]

The apparent contradiction of Fig. 3 and 4b, as the (Ca-FeSi + Enhancer) inoculation variant led simultaneously to the lowest amount of carbides and graphite, could result from the difficulties associated with the automatic image analysis. The probable cause was the result of trying to evaluate a ductile iron structure characterized by graphite nodules having a small size (Fig. 4a), that was typical for this inoculation variant. For this reason, when using a trap size of 5µm for graphite particles, it is highly possible that an important amount of nodules less than 5µm size were not included in this analysis.

Nodule counts are a complex parameter that can be greatly affected by cooling rate. Increased cooling rates typically produce higher graphite nodule counts, but conversely, free carbides are also promoted by high cooling rates. This investigation found that at the highest cooling rate in the wedge apex area, large amounts of free carbides formed. Also found was that high cooling rates had a significant effect on graphite nodule count (Figures 3 and 4).

The high level of carbides that formed in the apex for Ca,Ba and Ca,RE inoculation systems resulted in low nodule

counts. Higher graphitizing capacity was universally found for the Ca-FeSi and [Ca + Enhancer] inoculation variants. The Ca-FeSi and [Ca + Enhancer] inoculation variants both showed higher nodule counts in the high solidification cooling rate apex zone.

Decreasing the cooling rate as the distance from the apex increased (section size), led to decreased carbide levels and increased graphite amounts on all casting wedge sections. Nodule count also decreased at distances up to 10 mm from the apex (5mm section size). At distances greater than 10 mm from the apex, nodule count remained relatively constant, but within a wide range of 200 to 450 Nodules mm^{-2}, depending on the inoculation variant. In these experiments, the highest nodule count characterizes ductile iron inoculated with the lowest inoculant addition, the (Ca + Enhancer) variant, followed by the highest inoculant addition, the Ca-bearing 75% FeSi alloy. It appeared that the enhancing of the standard Ca-bearing 75% FeSi alloy inoculation intensity by the contribution of an addition of S, O and oxide-forming elements, in the form of the proprietary OS-IE alloy, was a better solution than the using of more expensive inoculating elements, such as REE. It was especially reflected by the obtained lowest carbides amount and the highest nodule count in the present ductile irons, characterized with REE_{re} levels less than 0.01% after Mg-treatment.

In actual foundry practice, graphite nodularity is typically used as a true measure of ductile iron quality. Over time, different expressions of graphite nodularity have been used. Generally, most all expressions refer to the ratio of nodular (spheroidal) particles compared to total particles in ductile iron structure. As flake (lamellar) graphite amounts are exempted, traditionally graphite nodularity is expressed as the ratio of nodular (spheroidal)/compacted (vermicular). As automated image analysis is used more and more to quantify the quality of ductile iron, determination of nodularity and nodule count has become very important. A recent publication[31] on the determination of nodularity and nodule count using image analysis pointed out the effect of several varying analytical parameters. This research showed important differences in graphite nodularity and nodule count can arise depending on the shape factors that are selected.

The graphs shown in Figure 5 compare the graphite nodularity (NG-SSF) values, calculated from Equation 2, for three levels of sphericity shape factors [SSF, Equation 1]. The data in all three graphs are for nodular (spheroidal) structures having SSF values between 0.5 to 1.0. Normally, as SSF values increase, the corresponding NG-SSF values decrease. Using a minimum sphericity shape factor SSF value of 0.5, more than 90% nodularity was observed for all of the tested irons, as shown in Figure 4. If the minimum limit of the shape factor is increased to a SSF value of 0.625, the nodularity appears to fall in the range of 80 to 95%, which would be typical of most ductile iron castings. Using the highest minimum shape factor SSF value of 0.8, corresponding to the highest compactness degree level for the graphite particles, the nodularity range fell to a 60 to 90% range. In many cases, this would be insufficient for some of the inoculated irons to be accepted as high performance ductile iron.

Solidification cooling rate, depending on the section size, had a complex action on the graphite nodularity. Generally, the lowest nodularity characterized graphite phase in the apex area, which solidified at the highest cooling rate, while the highest level of nodularity resulted for 5 to 6mm section size [10 to 12mm distance from the apex]. After that, the lowering of the cooling rate to the upper part of wedge casting affected graphite nodularity, but was dependent on the claimed graphite shape factor and inoculation variant. When the minimum value of SSF was 0.5, nodularity was not visibly influenced by the cooling rate, with only a slight dependence on the inoculation variant. When the minimum SSF values were 0.625 and 0.8, both the cooling rate and inoculant variant became important influencing factors, especially for SSF values of 0.8. Decreasing of the cooling rate generally decreased the graphite nodularity, becoming more pronounced for the highest level of graphite shape factor.

Inoculation can have a significant effect on graphite nodularity, especially if the minimum value of the Sphericity Shape Factor is 0.8 or higher. The experimental results showed that the highest nodularity resulted from inoculation with the 0.04wt.% [(Ca-FeSi + (OS-IE)] alloy variant (Fig. 6). Adding the proprietary inoculant enhancer (OS-IE) as a separate addition with the conventional Ca-FeSi alloy yielded reduced inoculant consumption levels [0.04wt.%] [Figs. 5

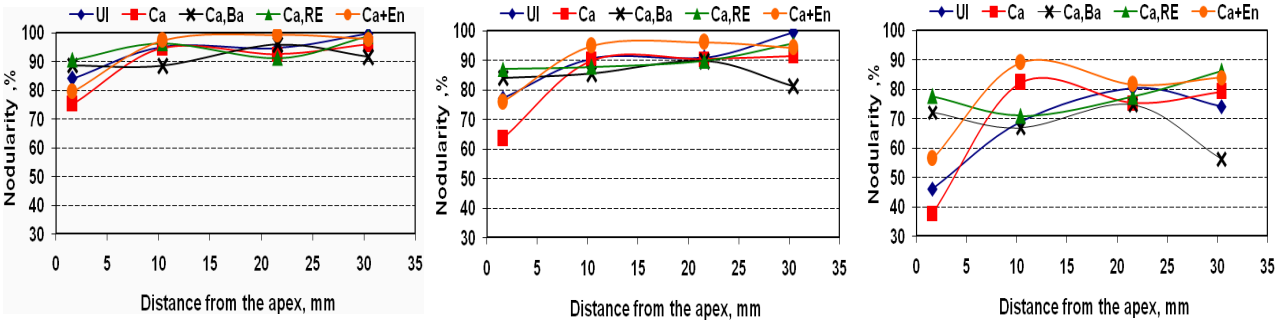

Fig. 5: Influence of the distance from the apex [W_3 wedge samples, ASTM A367] and inoculating elements on the graphite nodularity, depending on Sphericity Shape Factor [(a)-SSF=min. 0.5; (b)-SSF=min. 0.625; (c)-SSF=min.0.8] [Ca–0.18%Ca-FeSi; Ca,Ba–0.10%Ca,Ba-FeSi; Ca,RE–0.04%Ca,RE-FeSi; Ca+En–0.04% [3/4Ca-FeSi + ¼ OS-IE)]

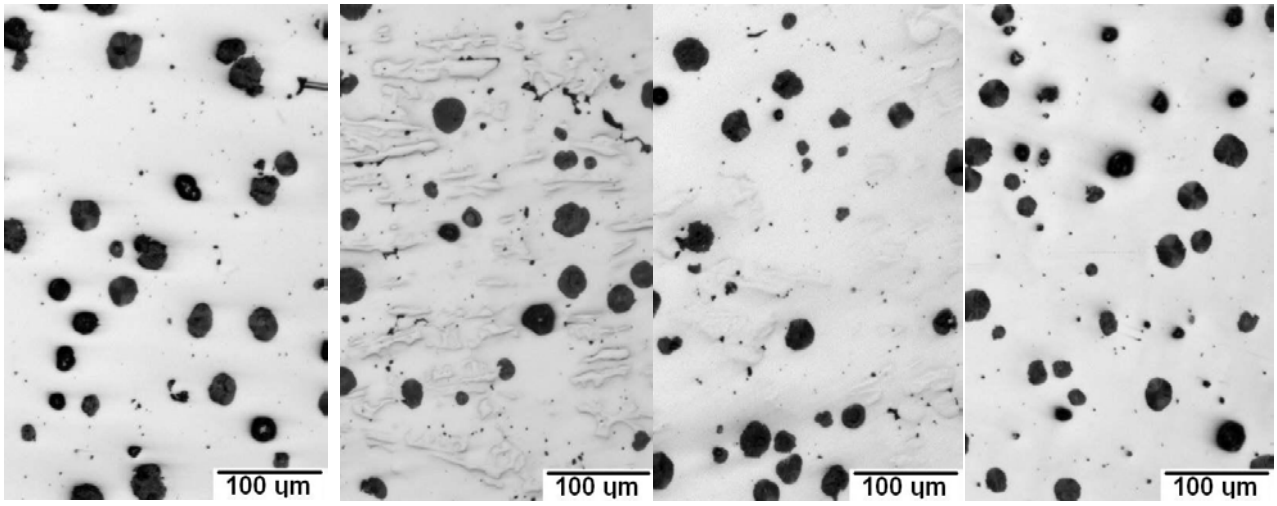

Fig. 6: Typical nodular graphite view at 10mm from the apex [5mm section size], W_3 wedge, ASTM A 367 [Ca – 0.18%Ca-FeSi; Ca,Ba – 0.10%Ca,Ba-FeSi; Ca,RE – 0.04%Ca,RE-FeSi; Ca+En – 0.04% [3/4Ca-FeSi + ¼ OS-IE)]

and 6]. Depending on which ever graphite shape factor was selected, the [(Ca-FeSi + (OS-IE)] inoculant variant produced 1.) 95% nodularity for SSF values were 0.5 minimum, 2.) nodularity was greater than 90% nodularity when SSF values were 0.625 minimum, and 3.) nodularity was greater than 80% nodularity when SSF values were 0.8 minimum.

It should be noted that the ability of this inoculation variant [(Ca-FeSi + (OS-IE)] to produce a graphite phase of maximum compactness is extremely beneficial for high ductility properties. Although excellent inoculation behavior was found for the Ca-FeSi inoculant variant, it required 450% larger in-mould additions to achieve results almost as good as the [(Ca-FeSi + (OS-IE)] variant. The Ca,Ba-FeSi inoculant variant provided the least chill reduction capability and produced satisfactory nodularity results only when SSF was less than 0.625. Intermediate chill reduction capability and nodularity results were obtained with the RE–0.04%Ca,RE-FeSi alloy variant.

The efficiency of the inoculation enhancer (OS-IE) used with Ca-FeSi, [(Ca-FeSi + (OS-IE)] has been substantiated with actual foundry production experience.[27] International Foundry X is a high-production automotive foundry that became concerned about rare-earth metal availability and the subsequent effect on the sky-rocketing cost of the rare earth-containing inoculant it had been using. Prior to changing the inoculation practice by adding separate additions of the inoculation enhancer (OS-IE) with Ca-FeSi, the tundish treated-Mg iron is transferred into unheated stopper rod pouring vessels where post-inoculation was performed using a proprietary rare earth inoculant containing sulphur and oxide surface treatments. After numerous qualification tests, which included 1.) in-depth thermal analysis, 2.) pouring test castings that had both thin sections and an isolated heavy section prone to shrinkage, and 3.) fading tests, this foundry made a complete change in their inoculation practice. Post inoculation is now done with the same alloy quantity, but the REE-inoculant has been replaced with a Ca-bearing FeSi alloy and OS-IE inoculant enhancer, used in a ratio of 3 to 1 respectively (the OS-IE is added separately to the un-heated pouring vessels). This combination of inoculants produced identical results to the more costly rare-earth inoculant. This foundry pours 400 tons ductile iron castings per day and estimates it is saving over US$8.00 per ton with the new inoculation procedure. On an annual basis, savings are estimated to be US$750,000 and the foundry reduced the need for REE addition.

Conclusions

1. It was found that in a relatively pure base iron, with low anti-nodularising trace elements (Thielman Factor K less than 0.8) the metal matrix and graphite phase characteristics are affected by (a) the solidification cooling rate, (b) post-Mg-treatment application and (c) inoculant type.
2. All of the modified Ca-bearing FeSi alloys showed improved inoculation capability, as incorporating either Ba or REE allowed a lower consumption of inoculants. For an in-mould technique and 0.10% Ca,Ba-FeSi or 0.04%Ca,RE-FeSi alloys, the chill tendency is practically at the same level as for 0.18%Ca-FeSi treatment.
3. The highest inoculation efficiency occurred when adding an oxy-sulphide inoculant enhancer alloy with 75% Ca-bearing FeSi [1:3 ratio]. This combination of additions was more effective than an equivalent addition of a REE-bearing, Ca-FeSi alloy or compared to the Ca,Ba-FeSi variant, but with a 60% lower alloy consumption, or the Ca-FeSi variant, with a 77% lower alloy consumption.
4. The [Ca-FeSi + OS-IE] inoculation variant resulted in the highest graphite nodularity, based on the imposed Sphericity Shape Factor SSF: greater than 95% for SSF values of 0.5 minimum, greater than 90% for SSF values of 0.625 minimum, and greater than 80% for SSF values of 0.8 minimum, despite being used as the lowest consumption level.

5. The enhancement of Ca-FeSi alloy inoculation potency by contributions of S, O and oxide-forming elements, proved to offer a better solution than the using of more expensive other inoculating elements, such as REE.
6. Should the level of REE in Mg-FeSi master alloys decrease because of price or availability in the future, modifying the basic charge along with selection of the proper inoculants will insure the production of high quality ductile irons castings. Inoculation enhancing by adding S, O and oxide-forming elements [such as OS-IE Enhancer] to commercial simple inoculants could be an alternative solution to REE presence in treatment alloys in ductile iron castings production.

References

1. M. Chisamera, I. Riposan, S. Stan and T. Skaland: Proc. 64th World Foundry Congress, Paris, France, CIATF, Sept. 2000, Paper R0 62.
2. I. Riposan, M. Chisamera, S. Stan, T. Skaland and M. Onsoien: *AFS Trans.*, 2001, 109, 1151-1162.
3. I. Riposan, M. Chisamera, S. Stan and T. Skaland: *Int. J. Cast Met. Res.*, 2003, 16 (1-3), 105-111.
4. I. Riposan, M. Chisamera, S. Stan and T. Skaland: Proc. AFS Cast Iron Inoculation Conference, Schaumburg, IL, USA, September 2005, AFS, 31-42.
5. I. Riposan, M. Chisamera, C. Hartung and D. White: *Mater. Sci. Technol.,* 2010, 26 (12), 1439-1447.
6. M.H. Jacobs, T.J. Law, D.A. Melford and M. Stowell: *Metal Technol.*, 1974, 490-500; 1976, 98-108.
7. T. Skaland: 'Nucleation Mechanism in Ductile Iron'. PhD Thesis, Trondheim, Norway, 1992.
8. R.L. Naro and J.F. Wallace: *AFS Trans.*, 1969, 77, 311; 1970, 78, 229.
9. K. Strande: Proc. 51st. Intern. Foundry Congr., Lisbon, Portugal, 1984.
10. I. Riposan, M. Chisamera and G. Simionescu: RO Patent No. 101339, 1988.
11. M. Chisamera and I. Riposan: *Advanced Materials Research,* Trans Tech. Publ., 1997, 4-5, 293-300.
12. M. Chisamera, I. Riposan and M. Liliac: Proc. INFACON7, Trondheim, Norway, 1995, 742-749.
13. M. Chisamera, I. Riposan and M. Barstow: Proc. AFS Cast Iron Int. Inoculation Conf., Chicago, IL, USA, April 1998, Paper no. 3.
14. I. Riposan, M. Chisamera, L. Sofroni, S. Stan and M. Liliac: Proc. 63rd World Foundry Congress, Budapest, Hungary, 1998; Kohaszat, 1999, 1, 11-18; 1999, 2, 59-65.
15. T. Skaland: U.S. Patent No.6,102,983, (August 15, 2000), International Patent W099/29911.
16. T. Skaland: Proc. 105th AFS Casting Congress, Dallas, USA, 2001, Paper 01-078.
17. J.K. Solberg and M.I. Onsoien: *Mater. Sci. Technol.*, 2001, 17, 1238–1242.
18. V. Igoraski and S. Okade: *Int. J. Cast Met. Res.*, 1998, 11, 83–88.
19. H. Nakae and Y. Igarashi: *Mater. Trans.,* 2002, 43(11), 2826–2831.
20. M.J. Lalich and J.R. Hitching: *AFS Trans.*, 1976, 84, 653–664.
21. I. Riposan, M. Chisamera, S. Stan and D. White: *AFS Trans.,* 2007, 115, 423-433.
22. M. Chisamera, I. Riposan, S. Stan and D. White: *Int. J. Cast Met. Res.*, 2009, 22(6), 401–410.
23. I. Riposan, M. Chisamera, S. Stan, P. Toboc, G. Grasmo, D. White, C. Ecob and C. Hartung: Proc. Keith Millis Symposium on Ductile Cast Iron, Las Vegas, NV, USA, Oct. 2008, DIS/AFS, 206–214; *J. Mater. Eng. Perform.*, 2011, 20 (1), 57-64.
24. R.L. Naro: U.S. Patents No. 6,293,988 B1, (September, 2001), No. 6,733,565 B1, No. 6,866,696B1.
25. R.L. Naro: *Foundry Management Technol.*, 2002, 20.
26. M. Chisamera, I. Riposan, S. Stan, C.B. Albu and R.L. Naro: *AFS Trans.*, 2007, 115, 481- 493.
27. R.L Naro, D.C. Williams, M. King and L. Basaj: *Foundry Manag. Technol.,* January 23, 2012.
28. I. Riposan, M. Chisamera, V. Uta, S. Stan, R.L. Naro and D.C. Williams: Proc. 2013 Keith Millis Symposium on Ductile Cast Iron, Nashville, TN, USA, October 2013, DIS/AFS, 256-275; *Int. J. Metalcasting*, 2014, 8 (2), 65-80.
29. I. Riposan, V. Uta, S. Stan, R.L. Naro and D.C. Williams: *AFS Trans.*, 2014, 122, Paper 14-004.
30. T. Thielman: *Giessereitechnik*, 1970, 1, 16-24.
31. S. Grenier, A. Bhattacharjee, R.B. Gundlach, B. Kroka, C. Labrecque and M. Riabow: Proc. 2013 Keith Millis Symposium on Ductile Cast Iron, Nashville, TN, USA, October 2013, DIS/AFS, 1-13.

Acknowledgment

The work has been funded by the Sectoral Operational Programme Human Resources Development 2007-2013 through the Financial Agreements POSDRU/159/1.5/S/132395 and POSDRU/159/1.5/S/134398. The authors would like to recognize and thank Dr. Rod Naro, ASI International Ltd, for partially supplying funding for the experiments and presentation at the SPCI10 Int. Symposium on the Science and Processing of Cast Iron, Mar del Plata, Argentina, 2014.